Available online at www.sciencedirect.com
ScienceDirect
Polyhedron 26 (2007) 4899–4907
POLYHEDRON
www.elsevier.com/locate/poly

5-Nitroaminotetrazole as a building block for extended network structures: Syntheses and crystal structures of a number of heavy metal derivatives

Sergey N. Semenov *, Andrey Yu. Rogachev, Svetlana V. Eliseeva, Yury A. Belousov, Andrey A. Drozdov, Sergey I. Troyanov

Department of Chemistry, Moscow State University, 119899 Moscow, Vorobjevy Gory, Russia

Received 16 April 2007; accepted 21 June 2007
Available online 22 August 2007

Abstract

The lead, mercury, copper and silver derivatives of 5-nitroaminotetrazole (5-H_2NATZ) were obtained by the reaction between the metal nitrate and potassium 5-nitroaminotetrazolate. The lead and mercury complexes were crystallized and characterized by single crystal X-ray diffraction. The lead complex has a polymeric structure formed by $(PbO_2)_n$ chains and anions of 5-NATZ, where each lead atom is surrounded by ten oxygen atoms. The mercury salt is constructed from neutral $(Hg–NATZ)_n$ chains, where the mercury atom has a linear coordination. The influence of chemical hardness and charge distribution on the reactivity and coordination properties of 5-NATZ was estimated based on density functional calculations. The thermal stability of the salts was also studied.

Keywords: Tetrazoles; DFT calculations; Network structures; Mercury complex; Lead complex

1. Introduction

In recent years, the synthesis of tetrazole-based network architectures has produced a great interest due to their various applications as zeolite-like, ion exchange, magnetic, non-linear optical and luminescent materials as well as for their interesting topologies [1–9]. Like small building units with different coordination properties, tetrazole derivatives can give a wide range of extended network structures, being a good model compound to understanding detailed interactions, complimentary and other controlling factors in network systems [10]. The majority of recent works about tetrazole complexes deals with in situ synthesis of tetrazol derivatives obtained from nitrile and azide compounds. In this way, 3D networks with interesting topologies were obtained from complexes of 5-methyl and ethyltetrazoles [2,6,9], different pyridyltetrazoles [4,7] and bis(tetrazolyl)amine [3]. In recent work 2-(1*H*-tetrazol-5-yl)pyrazine has been used to build H-bonded supramolecular structures [11].

Tetrazole derivatives are also important due to their high energetic properties. Different tetrazole derivatives such as salts of 5,5′-azotetrazole [12], the perchlorate and nitrate of 1,5-diaminotetrazole [13], and organic salts of nitrotetrazole [14] have been tested as potential materials for modifying the combustion rates of rocket propellants, as gas generators and explosive materials. Cationic tetrazol salts are also potential high energetic ionic liquids [15,16]. Such energetic properties along with controlled molecular architecture in combination with appropriate outer- and inner-sphere ligands, allow one to vary the physicochemical and explosive properties over a wide range.

5-H_2NATZ (5-nitroaminotetrazole) possesses excellent energetic properties amongst the simple tetrazole derivatives. It can be prepared by the relatively simple method described by Lieber et al. [17] (Scheme 1).

* Corresponding author. Tel.: +7 4959394549.
E-mail address: semenov@inorg.chem.msu.ru (S.N. Semenov).

0277-5387/$ - see front matter © 2007 Elsevier Ltd. All rights reserved.
doi:10.1016/j.poly.2007.06.035

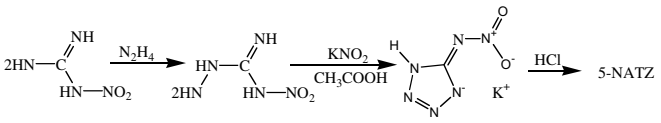

Scheme 1.

The latter was investigated in general, from the standpoint of its energetic properties. The thermal decomposition and crystal structure of 5-H_2NATZ have been described in detail in [18–20]. The heat of decomposition is equal to 3520 J/g [18], the calculated value of the heat of formation is approximately 500 kJ/mol [19–21]. Activation energies were calculated for 5-H_2NATZ and its mercury and lead salts [22]. The structural chemistry of alkaline metal and ammonium 5-nitroaminotetrazolates are well investigated. Crystal structures of $NH_4CN_6O_2H$ [23], $(NH_4)_2CN_6O_2$ [24], MCN_6O_2H (M = Cs [25], Na [26], Li [27]) $Rb_3(CN_6O_2)(CNNNO_2)\cdot H_2O$ [25] and the K^+ salt of 3-methyl-5-nitroaminotetrazole [28] have been reported. Complexes of 5-NATZ with transition metals are poorly studied, only the crystal structure of the nickel dimeric complex, $Ni_2(NH_3)_6(CN_6O_2)_2$ [29], has been determined. However, 5-H_2NATZ and its derivatives should be an interesting class of ligands, due to the following reasons: (i) 5-H_2NATZ is a dibasic acid that can be easily transformed into mono and di-substituted salts; (ii) anions of 5-NATZ have many sites for coordination by metal ions; and (iii) conjugated systems of five-member rings of tetrazoles can form π–π intermolecular interactions in the crystal structure to build extended 2D and 3D networks. It worth mentioning that the anionic form of tetrazole considered can be strictly controlled by using appropriate conditions. In this context, 5-NATZ is the perspective ligand for construction of high energetic network structures with a combination of physicochemical and explosive properties.

In this work, we present the syntheses and crystal structures of the mono-substituted complex of lead(II) as well as a disubstituted complex of mercury(II). Furthermore, the interpretation of the coordination mode through electronic features of 5-NATZ and its mono- and dianion was performed by means of theoretical modelling.

2. Experimental

2.1. Materials and methods

The guanidine carbonate, potassium nitrite, mercury, silver, lead and copper nitrates were obtained from the Aldrich Chemical Company Ltd. and Fluka, and were used without purification. *N*-Nitro-*N*-aminoguanidine was obtained from nitroguanidine [30], which was obtained from guanidine nitrate [31]. Chemical analyses of the samples dried to a constant weight were performed with a Fisons Instruments 1108 CHNS-O Elemental analyzer. IR spectra in the range 4000–400 cm^{-1} were recorded on a Perkin–Elmer System 2000 FT-IR spectrometer. Decomposition temperatures were determined on an IA 8100 Electrothermal instrument. Lead and silver contents were determined by weight analysis in the forms of $PbMoO_3$ and AgBr. The copper content was determined by iodometric titration.

2.2. Synthesis

2.2.1. Synthesis of potassium 5-nitroaminotetrazolate (*1*)

Complex **1** was prepared by interaction of *N*-nitro-*N*-aminoguanidine with KNO_2 and acetic acid, as described in [17]. Yield: 65%. $T_{decom.} = 248$ °C. *Anal.* Calc. for $KHCN_6O_2$: C, 7.14; H, 0.60; N, 49.98. Found: C, 6.92; H, 0.53; N, 50.13%. IR (Nujol, cm^{-1}): 2726 (*ν*N–H), 1544 (*ν*C–N), 1450 (*ν*N–O), 1318 (*ν*N–NO_2),1224 (*ν*C–N–NO_2), 1146 (*ν*N–N), 1094, 1058 (*ν*N–N), 1030 (*δ*N–H), 998 (*ν*N–N), 864, 774 (*δ*N–NO_2), 746, 698 (*δ*N–H), 462, 418 (*ν*O–K).

2.2.2. Synthesis of bis-potassium 5-nitroaminotetrazolate (*2*)

Complex **2** was obtained by reaction of equimolar amounts of **1** and KOH. Yield: 85%. $T_{decom.} = 400$ °C. *Anal.* Calc. for $K_2CN_6O_2$: C, 5.82; N, 40.78. Found: C, 5.54; N, 40.33%. IR (Nujol, cm^{-1}): 1396 (*ν*N–NO_2), 1294 (*ν*N–O), 1146 (*ν*N–N), 1028 (*ν*C–N), 1010 (*ν*N–N), 862 (*δ*C–N–NO_2), 462, 418 (*ν*O–K).

2.2.3. Synthesis of 5-NATZ (*3*)

Compound **3** was prepared by the procedure described in [17]. The pure product was isolated by extraction with diethyl ether. Yield: 48%. *Anal.* Calc. for $H_2CN_6O_2$: C, 9.23; H, 1.55; N, 64.61. Found: C, 9.11; H, 1.63; N, 64.62%.

2.2.4. Synthesis of lead 5-nitroaminotetrazolate (*4*)

To a solution of $Pb(NO_3)_2$ (0.44 g, 0.625 mmol) in 3 ml of water, a solution of 0.21 g (1.25 mmol) of **1** in 3 ml of water was added. After 1 h, salt **3** started to crystallize as large prisms. The crystals were separated by filtration. Yield: 76%. $T_{decom.} = 230$ °C. *Anal.* Calc. for $PbH_2C_2N_{12}O_4\cdot 4H_2O$: Pb, 38.56; C, 4.47; H, 1.88; N, 31.28. Found: Pb, 38.47; C, 4.68; H, 1.74; N, 31.13%. IR (Nujol, cm^{-1}): 3376 (*ν*O–H), 2726 (*ν*N–H), 1650, 1526 (*ν*C–N), 1462(*ν*N–O), 1342 (*ν*N–NO_2),1254 (*ν*C–N–NO_2), 1158 (*ν*N–N), 1120, 1066 (*ν*N–N), 1034 (*δ*N–H), 996 (*ν*N–N), 866, 770 (*δ*N–NO_2), 740, 700 (*δ*N–H), 416.

2.2.5. Synthesis of copper 5-nitroaminotetrazolate (*5*)

To a solution of $Cu(NO_3)_2\cdot 3H_2O$ (0.242 g, 1 mmol) in 2 ml of water, a solution of 0.168 g (1 mmol) of **1** in 3 ml of water was added. After 5 h, complex **3** precipitated as a dark-green fine crystallized powder, and was separated by filtration. Yield: 69%. $T_{decom.} = 240$ °C. *Anal.* Calc. for $CuCN_6O_2(H_2O)_3$: Cu, 25.92; C, 4.86; H, 2.43; N,

34.01. Found: Cu, 26.13; C, 4.76; H, 2. 32; N, 34.07%. IR (Nujol, cm^{-1}): 3380 (νO–H), 2735 (νN–H), 1630, 1500 (νC–N), 1406 (νN–NO_2), 1298, 1268 (νN–O), 1182 (νN–N), 1020 (νN–N), 1010 (νN–N), 872 (δC–N–NO_2), 748 (δC–N–C), 560, 492.

2.2.6. Synthesis of silver 5-nitroaminotetrazolate (6)

A solution of 0.168 g (1 mmol) of **1** in 3 ml of water was added to solution of $AgNO_3$ (0.34 g, 1 mmol) in 1 ml of water. A white precipitate formed immediately. This substance was separated by filtration. Yield: 83%. $T_{decom.}$ = 345 °C. *Anal.* Calc. for $Ag_2CN_6O_2(H_2O)_3$: Ag, 54.18; C, 3.01; H, 1.50; N, 21.05. Found: Ag, 53.65; C, 2.94; H, 1.67; N, 21.28%. IR (Nujol, cm^{-1}): 3650 (νO–H), 1612, 1546 (νC–N), 1350 (νN–NO_2), 1316 (νN–O), 1238 (νC–N), 1054 (νN–N), 1002 (νN–N), 880 (δC–N–NO_2), 760 (δC–N–C), 736.

2.2.7. Synthesis of mercury 5-nitroaminotetrazolate (7)

To a solution of $Hg(NO_3)_2$ (0.34 g, 1 mmol) in 1 ml of water, a solution of 0.168 g (1 mmol) of **1** in 3 ml of water was added. A white precipitate formed immediately. This substance was separated by filtration. Yield: 83%. $T_{decom.}$ = 165 °C. *Anal.* Calc. for $HgCN_6O_2(H_2O)_2$: C, 3.29; H, 1.11; N, 23.05. Found: C, 3.24; H, 1.23; N, 22.87%. IR (Nujol, cm^{-1}): 3450 (νO–H), 1618, 1488 (νC–N), 1328 (νN–NO_2), 1286 (νN–O), 1184 (νC–N), 1026 (νN–N), 962 (νN–N), 863 (δC–N–NO_2), 756 (δC–N–C).

2.3. Single-crystal X-ray structure determination

Single crystals of **4** suitable for X-ray structure determination were obtained by slow evaporation of the water solution. The crystals of **7** were grown by slow diffusion of mercury(II) nitrate through silica gel containing potassium 5-nitroaminotetrazolate.

Data collection for crystals of **4** was carried out at room temperature on a four-cycle diffractometer using graphite-monochromated Mo Kα radiation (λ = 0.71973 Å), whereas data collection for **7** was carried out on a Stoe IPDS diffractometer (Imaging Plate Detector System) with graphite-monochromated Mo Kα radiation (λ = 0.71073 Å) at 183(2) K using a cold N_2-gas stream. The direct method was used to solve the crystal structures by applying the software options of the program SHELXS-97. The structure refinement was performed with the program SHELXL-97. Non-hydrogen atoms were refined anisotropically by full-matrix least-squares techniques based on F^2. The hydrogen atoms of organic groups were placed in calculated positions within a riding model approximation with a fixed temperature factor. Hydrogen atoms of water molecules were located based on the difference electron-density maps and were refined isotropically with a fixed bond length. Twining was observed for the crystal of **7**, the twining matrix was calculated using the PLATON program. Details of data collection and refinement are given in Table 1.

Table 1
Crystallographic data and details of structure refinements for **4** and **7**

Formula	$C_2H_{10}N_{12}O_8Pb$	$HgCN_6O_4H_4$
Formula weight	537.35	365.41
Crystal system	orthorhombic	monoclinic
Space group	*Pbcn*	$P2_1/n$
a (Å)	20.816 (4)	14.958 (3)
b (Å)	9.630 (2)	6.590 (1)
c (Å)	6.273 (1)	14.958 (3)
β (°)	90	111.99 (3)
V (Å^3)	1257.5 (4)	1367.1 (5)
Z	4	8
D_{calc} (Mg/m^3)	2.796	3.500
T (K)	150	150
F(000)	976	960
Crystal dimensions (mm)	0.60 × 0.40 × 0.30	0.1 × 0.05 × 0.05
Θ_{max} (°)	28.27	27.48
Reflections collected	3124	6868
Independent reflections	1562	3036
Parameters	109	198
Goodness-of-fit	1.081	0.905
R_1	0.0316	0.0582
wR_2 (F^2)	0.0715	0.1427
Largest difference in peak and hole (e Å^{-3})	2.593 and −1.579	2.301 and −4.282

2.4. Calculation details

Full geometry optimization of the molecular structures were performed at the DFT level of theory using the hybrid Perdew–Burke–Ernzerhof parameter free exchange-correlation functional (PBE0) [32–34] as it is implemented in the PC GAMESS [35] version of the GAMESS-US [36] program package. Standard triple-split 6-311G(d,p) basis sets were used for all atoms of the systems under consideration. Geometry optimization of all the molecules was performed without any symmetry constrains (C_1 point group). The gradient norm was taken to be 10^{-5} a.u. The true minimum was controlled by the Hessian matrix and, as a consequence, harmonic frequencies calculation. The lack of imaginary frequencies indicates that the true minimum was achieved.

Based on the optimized geometry configurations, natural bond orbital (NBO) analysis [37,38] was performed for all systems. Computed data were visualized with help of the CHEMCRAFT program package [39].

In accord with Pearson [40], the chemical hardness (η) can be calculated by the following formula:

$$\eta = \frac{1}{2}\left(\frac{\partial^2 E}{\partial N^2}\right)_v = \frac{1}{2}\left(\frac{\partial \mu}{\partial N}\right)_v = \frac{1}{2}(I - A)$$

where I – ionization potential, A – electron affinity, E – the energy of N-electrons system, N – amount of electrons in the molecule, v – external potential, and μ – chemical potential. However, the Koopmans theorem allows the estimation of the hardness by using only orbital energies of the highest occupied molecular orbital (HOMO) and the lowest unoccupied molecular orbital (LUMO) of the molecule in its ground state as follows:

$$\eta \approx -\frac{1}{2}(\text{HOMO–LUMO})$$

Applicability of the Koopmans theorem to DFT MOs was found and confirmed by Baerends and co-workers [41] and Stowasser and Hoffmann [42].

3. Results and discussion

Potassium 5-nitroaminotetrazolate, obtained from guanidine carbonate, was used as the starting material. Other salts were obtained from the potassium salt **1** and the corresponding metal nitrates in water solution in accordance with the following reactions:

$$2KHCN_6O_2 + Pb(NO_3)_2 = Pb(HCN_6O_2)_2(H_2O)_4 + 2KNO_3$$

$$KHCN_6O_2 + Cu(NO_3)_2 = Cu(CN_6O_2)(H_2O)_3 + KNO_3 + HNO_3$$

$$KHCN_6O_2 + 2AgNO_3 = Ag_2(CN_6O_2)(H_2O)_3 + KNO_3 + HNO_3$$

$$KHCN_6O_2 + Hg(NO_3)_2 = [Hg(CN_6O_2)(H_2O)_2]_n + KNO_3 + HNO_3$$

The main difference between these reactions is that lead forms a mono-substituted salt, while copper, mercury and silver form di-substituted ones. It reflects the great affinity of Cu^{2+}, Hg^{2+} and Ag^{+} to soft ligands, and the propensity of silver to form completely substituted salts. The silver salt has high chemical stability and cannot be destructed by boiling with concentrated nitric acid. All the transition metal salts considered contain water molecules of crystallization. The hydrate composition has been calculated from the elemental analysis. In the case of lead and mercury derivatives, it was further confirmed by the crystal structure determinations.

IR spectra of 5-NATZ and alkali metal salts have been fully described previously [25]. Coordination of the ligand by a metal ion leads to an increase in the stretching vibrations in which atoms of the nitro-group are involved (Table 2).

Stretching displacements in the lead salt are in accordance with its crystal structure, where the metal atom is coordinated by the NO_2 group. Since the nitro-group is fixed, the energy of the stretching vibrations of the N–NO_2 and C–N–NO_2 fragments increases. There are two bands involving NO_2 asymmetric stretching in the copper complex.

Complex **4** crystallizes in the orthorhombic space group *P*bcn with four molecules in the unit cell. This compound has a polymeric structure formed by chains of $(PbO_2)_n$ and anions of 5-NATZ. The coordination number of lead is found to be 10. The lead ion is bound with three different types of oxygen atoms (Fig. 1): (i) oxygen atoms from bridging water molecules, (ii) oxygen atoms from terminal water molecules, and (iii) oxygens from nitro-groups.

The coordination polyhedron can be derived from the icosahedron by removal of two apexes with subsequent compression. The Pb–O bond lengths are in the range 2.653(5) to 2.888(5) Å (Table 3).

The Pb–O(terminal water) distance is equal to 2.653(5) Å, while the Pb–O(NO_2) bond length is 2.888(5) Å. The average Pb–O distance is 2.764(5) Å, being slightly greater than that in $Pb(CH_3COO)_2(H_2O)$, 2.742(6) Å [43], which has a similar polymeric crystal structure.

The anion of 5-NATZ in **4** is found to be monodeprotonated. Bond lengths in the ligand are similar to those for $MHCN_6O_2$, M = Li, Na, Cs [22–24]. The main difference between the 5-nitroaminotetrazolate anion in the lead salt and in alkali metal salts is observed for the bond lengths in the nitro group. The distances considered are significantly different (1.255(5) and 1.283(5) Å), and are longer than those in the case of $CsHCN_6O_2$ (1.243(5) and 1.260(5) Å). The latter can be the result of the coordination of the oxygen atoms with lead. The oxygen atom involved in the shortest Pb–O distance forms the longest N–O bond. The distance C(1)–N(2) (1.370(5) Å) shows the best correlation with the nitro-iminium form of the ligand [15,26]. Hydrogen atoms are connected to the N(6) nitrogen atom.

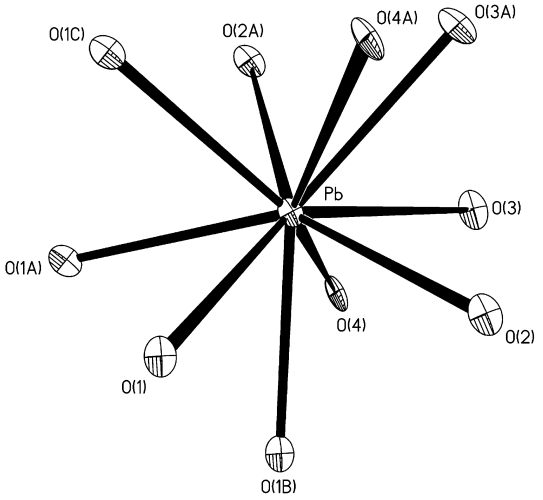

Fig. 1. Coordination environment of the lead ion.

Table 2
Frequencies of vibrational modes in metal complexes of 5-NATZ

	NO_2 asymmetric stretch	N–NO_2 stretch	C–N–NO_2 asymmetric stretch	N_3–N_4 stretch	N_2–N_3 stretch	C–N–NO_2 bending
$KHCN_6O_2$	1450	1318	1224	1058		
$Pb(HCN_6O_2)_2$	1460	1342	1254	1066		
$K_2CN_6O_2$	1294	1396			1010	862
$Ag_2CN_6O_2$	1316	1350			1002	880
$CuCN_6O_2$	1298, 1268	1406			1020	872
$HgCN_6O_2$	1286	1328			1026	863

Table 3
Selected bond lengths (Å) and angles (°) for $Pb(CHN_6O_2)_2(H_2O)_4$

Bond lengths (Å)		Bond angles (°)	
Pb–O(1)	2.888(5)	O(1)–Pb–O(2)	45.5(1)
Pb–O(2)	2.753(5)	O(1)–Pb–O(3)	62.5(1)
Pb–O(3)	2.784(5)	O(1)–Pb–O(3a)	122.9(2)
Pb–O(3a)	2.741(5)	O(1)–Pb–O(4)	99.4(2)
Pb–O(4)	2.652(5)	O(2)–Pb–O(3)	88.1(1)
O(2)–N(6)	1.283(7)	O(2)–Pb–O(3a)	144.1(2)
O(1)–N(6)	1.255(7)	O(2)–Pb–O(4)	71.9(2)
N(6)–N(5)	1.311(8)	O(3)–Pb–O(3a)	63.1(2)
N(5)–C(1)	1.370(8)	O(3)–Pb–O(4)	73.0(2)
N(4)–C(1)	1.328(8)	O(3a)–Pb–O(4)	79.0(1)
N(4)–N(3)	1.352(7)	N(6)–O(2)–Pb	100.5(4)
N(3)–N(2)	1.302(7)	O(1)–N(6)–O(2)	118.8(5)
		O(1)–N(6)–N(5)	125.1(6)
		O(2)–N(6)–N(5)	116.2(5)
		N(6)–N(5)–C(1)	115.7(6)
		C(1)–N(4)–N(3)	106.7(5)
		N(2)–N(3)–N(4)	110.8(5)
		N(3)–N(2)–N(1)	106.6(5)
		N(2)–N(1)–C(1)	108.6(5)
		N(4)–C(1)–N(1)	107.2(6)
		N(4)–C(1)–N(5)	119.7(6)
		N(1)–C(1)–N(5)	133.1(6)

Intramolecular and intermolecular hydrogen bonds are present in the crystal (Fig. 2); the former being observed between the O(4) atom and N(6) atom, the N(6)···O(4) distance is equal to 2.599(6) Å. Each 5-nitroaminotetrazolate ion is connected with a water molecule and adjacent ligands through five hydrogen bonds. All nitrogen atoms except N(2) and N(1) take part in hydrogen bonding. The intermolecular hydrogen bonds are characterized by the distances N–N 2.705(6) Å, N–O 2.828(6) Å and O–O 2.828(6) Å.

$(PbO_2)_n$ chains are stacked in the plane *bc* and form layers consisting only of lead ions and water molecules. 5-NATZ anions are located between the layers (Fig. 3). They

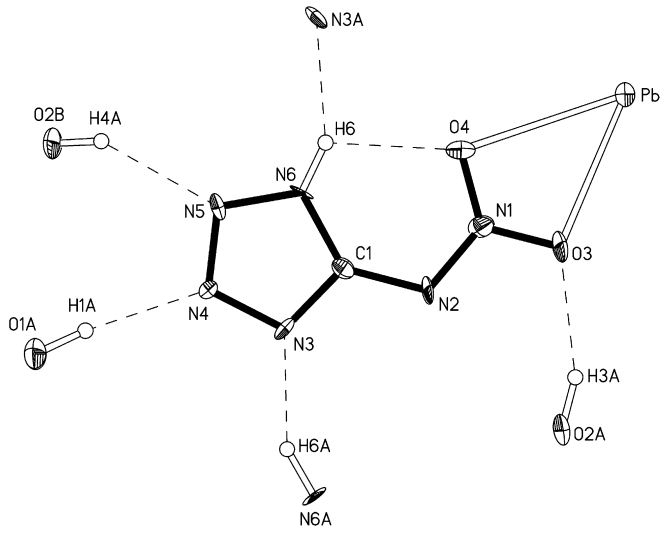

Fig. 2. System of hydrogen bonds around the 5-nitroaminotetrazolate ion, hydrogen bonds are shown as dashed lines.

are linked with lead by Pb–O bonds and are held together by hydrogen bonds, as described in the previous paragraph, and by stacking interactions. The distances between the planes of the tetrazole rings are equal to 3.143(6) Å. From such a point of view, the crystal structure of **4** has a hybrid structure that can be described as an intermediate step between an organometallic coordination polymer and an organic–inorganic hybrid material [44].

The polymeric crystal structure of **7** consists of infinite chains, $[–Hg–CN_6O_2–]_n$, fragments of which are presented in Fig. 4. The formal coordination number of mercury is equal to six. At the same time, the two Hg–N distances are significantly shorter than the Hg–O distances, 2.05(2) Å versus 2.60(2)–2.71(2) Å, respectively. In accord with these, the coordination geometry of mercury can be better described as linear, the N(3)–Hg–N(9) angle is 169° (Table 4). The Hg–N bond lengths are equivalent in the range of standard deviations, its value of 2.05(2) Å is slightly smaller than that for mercury nitrotetrazolate [45]. The difference in length of Hg–O and Pb–O bonds is due to the smaller radius of the Hg atom [46].

The structure of the $5\text{-}NATZ^{2-}$ anion shows differences from the corresponding structure in the alkali metal salts, Ni salt and the calculated geometry. Nitrogen atoms N(3) and N(6) have long N–N (1.40(2) Å) and C–N (1.35(2)–1.42(2) Å) bonds. These lengths are closer to single N–N and C–N bonds and consequently the Hg–N bonds have strong covalent character.

The $[–Hg–CN_6O_2–]_n$ chains are connected by bridged water in the 3D-network, Fig. 5. An extended networks of hydrogen bonds are observed in the crystal structure of the mercury derivative of 5-NATZ.

We have provided theoretical calculations on the equilibrium geometry, charge distribution (Figs. 8a–8c) and chemical hardness of $5\text{-}H_2NATZ$, $5\text{-}HNATZ^-$ and $5\text{-}NATZ^{2-}$ (Table 5) for interpretation of X-ray data and for in-depth consideration of 5-nitroaminotetrazolate coordination properties (for further details see Supplementary material). General numerations of the 5-NATZ atoms in this part are reflected in Fig. 6, and the main possible coordination modes are presented in Fig. 7.

Equilibrium geometrical parameters (Tables S1–S3) are in good agreement with the experimental X-ray diffraction data of $5\text{-}H_2NATZ$ [18] and its salts [25]. The C–N(2) distances, 1.307 and 1.349 Å for $5\text{-}H_2NATZ$ and $5\text{-}HNATZ^-$, respectively, confirm the nitroimino structure of this form. This distance in $5\text{-}NATZ^{2-}$ is 1.394 Å, being closer to the nitroamino form.

Charge distribution in $5\text{-}H_2NATZ$ shows a general pattern in which negative charges are concentrated on the oxygen atoms of the nitro group and the nitrogen atoms N(3) and N(6), but these nitrogen atoms are connected with hydrogens and consequently cannot be coordinated by metal. Therefore, neutral $5\text{-}H_2NATZ$ can really coordinate only through the oxygen atoms, type 1, 6. One hydrogen atom is omitted in the mono-deprotonated form $5\text{-}HNATZ^-$, enabling chelating coordination, type 2. The

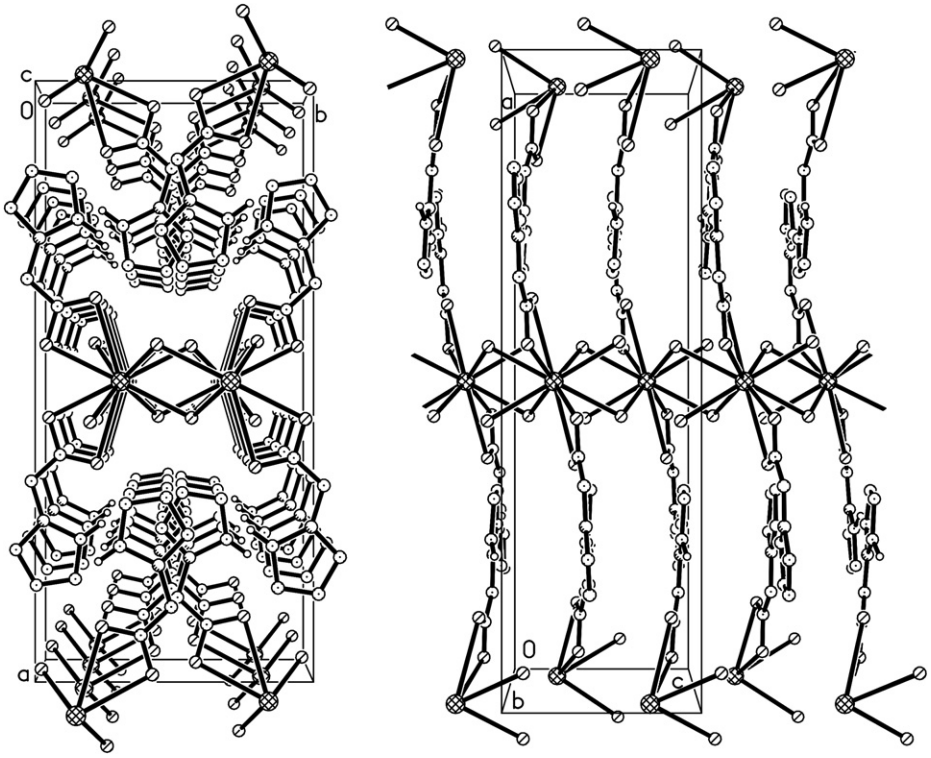

Fig. 3. Packing of $Pb(CHN_6O_2)_2(H_2O)_4$.

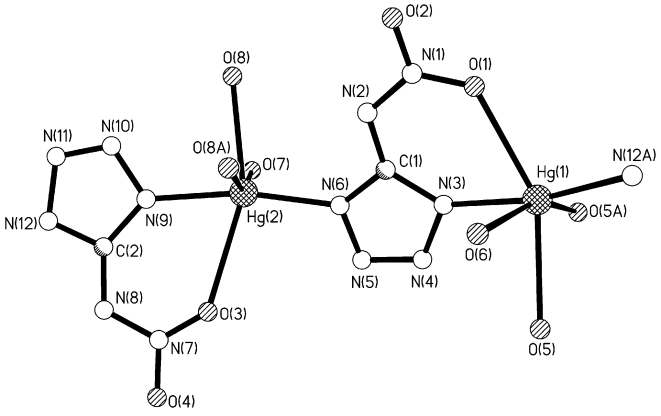

Fig. 4. Fragment of chain in **7**.

Table 4
Selected bond lengths (Å) and angles (°) for $[Hg(CN_6O_2)(H_2O)_2]_n$

Bond lengths (Å)		Bond angles (°)	
Hg(1)–N(3)	2.06(2)	N(3)–Hg(1)–N(12)	168.9(9)
Hg(1)–N(12)	2.05(2)	N(3)–Hg(1)–O(1)	70.4(8)
Hg(1)–O(1)	2.63(2)	N(3)–Hg(1)–O(5)	88.7(8)
Hg(1)–O(5)	2.60(2)	N(12)–Hg(1)–O(5)	101.9(8)
Hg(1)–O(5a)	2.71(2)	N(3)–Hg(1)–O(5a)	88.8(8)
Hg(1)–O(6)	2.70(2)	N(3)–Hg(1)–O(6)	84.6(8)
Hg(2)–N(6)	2.10(2)	N(9)–Hg(2)–N(6)	168.9(9)
Hg(2)–N(9)	2.07(2)	N(9)–Hg(2)–O(3)	70.4(8)
Hg(2)–O(3)	2.64(2)	N(9)–Hg(2)–O(8)	87.6(7)
Hg(2)–O(7)	2.65(2)	N(6)–Hg(2)–O(8)	103.5(7)
Hg(2)–O(8)	2.52(2)	N(9)–Hg(2)–O(7)	88.0(7)
Hg(2)–O(8a)	2.70(2)	N(9)–Hg(2)–O(8a)	91.2(7)

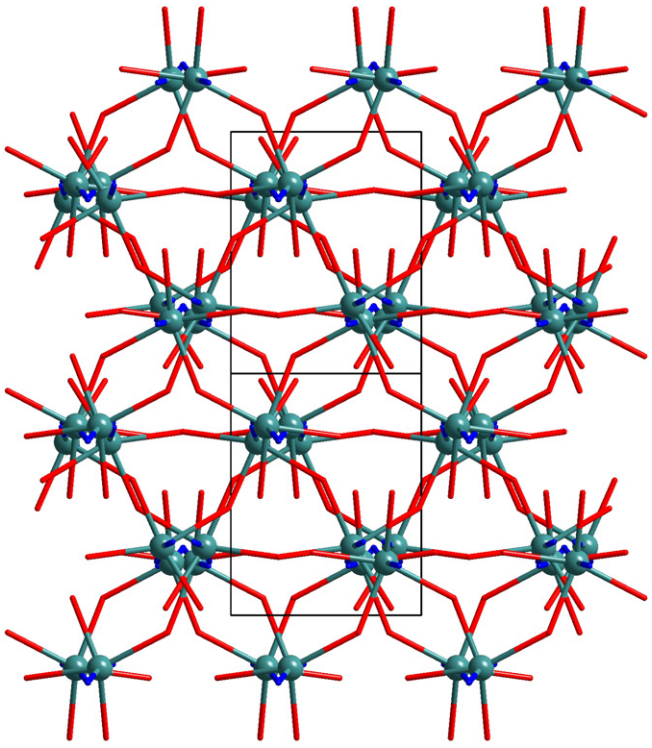

Fig. 5. Packing diagram of **7**, view along chains. Atoms, which are not connected with mercury, are omitted for clarity.

negative charges on N(4) and N(5) are increased relative to 5-H_2NATZ, but coordination through these nitrogen atoms is not probable in this case. The di-deprotonated form of

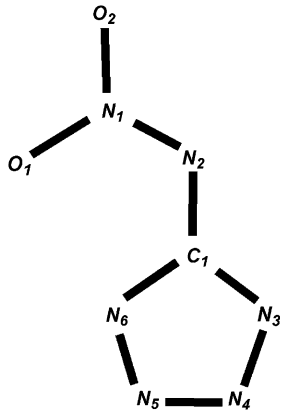

Fig. 6. Numeration scheme for 5-NATZ.

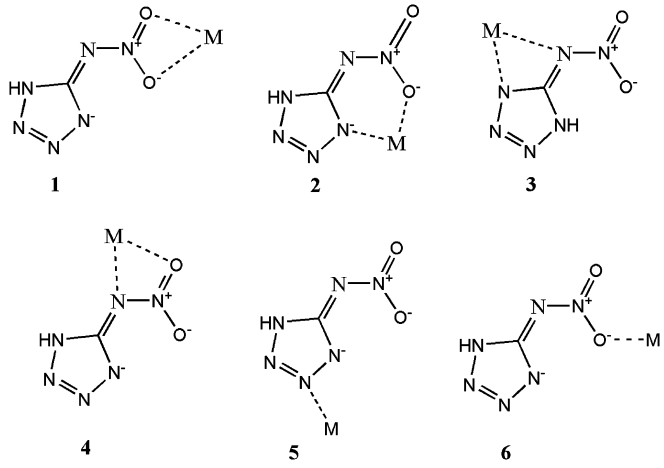

Fig. 7. Possible coordination modes for 5-nitroaminotetrazolates.

5-NATZ^{2-} shows the maximum possible coordination types, the negative charges on N(4) and N(5) continue to increase and that makes coordination through these atoms possible, e.g. as reported for the nickel derivative [29].

The hardness of the system decreases when we pass from the neutral to the di-deprotonated form, and it can lead to

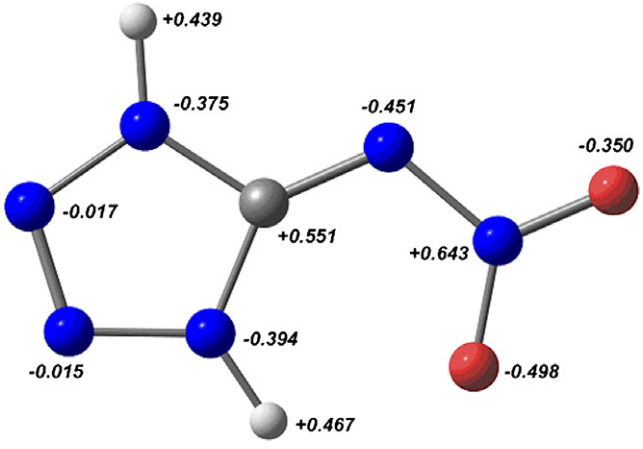

Fig. 8a. Charge distribution scheme for 5-H_2NATZ.

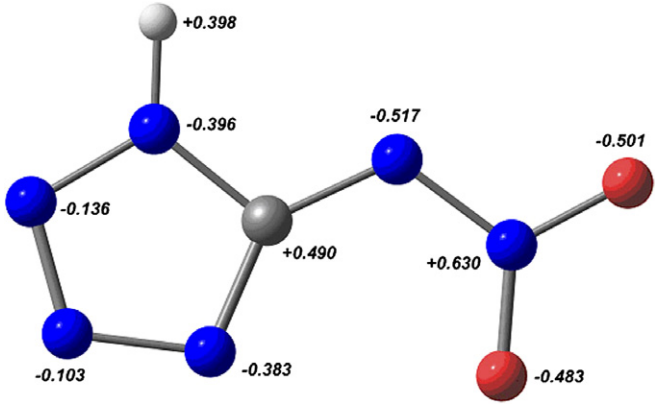

Fig. 8b. Charge distribution scheme for 5-HNATZ^{-}.

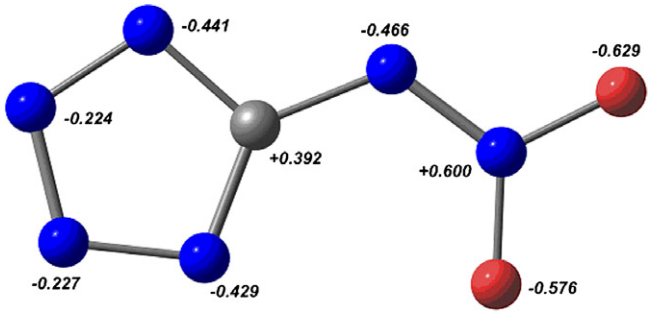

Fig. 8c. Charge distribution scheme for 5-NATZ^{2-}.

Table 5
Hardness of systems considered

System	Hardness (eV)
5-H_2NATZ	3.08
5-HNATZ^{-}	2.86
5-NATZ^{2-}	2.76

a preferred formation of di-substituted complexes in the case of soft metals such as silver and mercury. In this work such a tendency was illustrated with the structures of the lead and mercury derivatives. Interplay of the values of ionic radii and effective positive charge may play an important role in defining the coordination environment (CN Pb = 10, CN Hg = 6). In our opinion, there are two main reasons why the coordination numbers of lead and mercury differ: (i) the ionic radius of mercury is smaller than that of lead; (ii) the effective positive charge of the Hg atom is lowered due to the mostly covalent character of the Hg–N bond.

The temperatures of decomposition of the salts were determined (Table 6). The tendencies which were found for alkali metal salts [22] are also retained for the salts of heavy metals. The temperature of decomposition of the mono-substituted derivative salt is 1.5 times lower than

Table 6
Temperatures of onset of exothermic decomposition

Substance	T (°C)
$KHCN_6O_2$	245
Pb $(HCN_6O_2)_2$	230
$K_2CN_6O_2$	400
$Ag_2CN_6O_2$	345
$CuCN_6O_2$	240
$HgCN_6O_2$	165

that for the di-substituted silver one. The low temperature of decomposition of the copper(II) salt can be caused by the catalytic properties of the copper ion in oxidation reactions.

4. Conclusion

In this work, we showed the possibility of building chain-like extended networks using 5-nitroaminotetrazole (5-NATZ) as a ligand, with examples of lead and mercury salts. Calculations of charge distribution and chemical hardness of the systems showed that soft metal ions should give completely replaced salts with N-coordination. On the other hand, a hard metal can form acidic salts with O-coordination. This can be justified based on the crystal structures presented here. Both structures are polymeric, but the lead structure consists of $(PbO_2)_n$ chains with 5-HNATZ$^-$ acting as a terminal ligand coordinated through oxygen atoms. At the same time, use of the mercury ion gave rise to only the completely replaced salt consisting of $[–Hg–CN_6O_2–]_n$ chains with strongly covalent Hg–N bonds. The crystal structures of these salts give information about their potential applications, such as initiators for explosive materials. The lead derivative includes strongly coordinated water molecules that probably cannot be eliminated by heating in a vacuum. Thus, the lead salt is not a perspective initiator. Water molecules in mercury salt are weakly connected with the metal and are likely to be eliminated by heating in a vacuum. The anhydrous compound should exhibit better explosive properties.

Appendix A. Supplementary material

CCDC 626662 and 639048 contain the supplementary crystallographic data for **4** and **7**. These data can be obtained free of charge via http://www.ccdc.cam.ac.uk/conts/retrieving.html, or from the Cambridge Crystallographic Data Centre, 12 Union Road, Cambridge CB2 1EZ, UK; fax: (+44) 1223-336-033; or e-mail: deposit@ccdc.cam.ac.uk. Cartesian coordinates for all the calculated molecules; full sets of both experimental and theoretical geometrical parameters for all the molecules; full sets of NBO atomic charges in all the computed molecules; table with absolute energies for all the calculated molecules. Supplementary data associated with this article can be found, in the online version, at doi:10.1016/j.poly.2007.06.035.

References

[1] P.J. Koningsbruggen, Y. Garcia, H. Kooijman, A.L. Spek, J.G. Haasnoot, O. Kahn, J. Linares, E. Codjovi, F. Varret, J. Chem. Soc., Dalton Trans. (2001) 466.
[2] X.-M. Zhang, Y.-F. Zhao, H.-S. Wu, S.R. Batten, S.W. Ng, J. Chem. Soc., Dalton Trans. (2006) 3170.
[3] M. Friedrich, J.C. Galvez-Ruiz, T.M. Klapoetke, P. Mayer, B. Weber, J. Weigand, Inorg. Chem. 44 (2005) 8044.
[4] R.-G. Xiong, X. Xue, H. Zhao, X.-Z. You, B.F. Abrahams, Z.-L. Xue, Angew. Chem., Int. Ed. 41 (2002) 3800.
[5] X.-S. Wang, Y.-Z. Tang, X.-F. Huang, Z.-R. Qu, C.-M. Che, P.W.H. Chan, R.-G. Xiong, Inorg. Chem. 44 (2005) 5278.
[6] T. Wu, B.-H. Yiand, D. Li, Inorg. Chem. 44 (2005) 4130.
[7] P. Lin, W. Clegg, R.W. Harrington, R.A. Henderson, J. Chem. Soc., Dalton Trans. (2005) 2388.
[8] M. Dinca, A.F. Yu, J.R. Long, J. Am. Chem. Soc. 128 (2006) 8913.
[9] T. Wu, R. Zhou, D. Li, Inorg. Chem. Commun. 9 (2006) 341.
[10] A.J. Blake, N.R. Champness, P. Hubberstey, W.-S. Li, M.A. Withersby, M. Schröder, Coord. Chem. Rev. 183 (1999) 117.
[11] J.-R. Li, X.-H. Bu, G.-C. Jia, S.R. Batten, J. Mol. Struct. 828 (2007) 142.
[12] A. Hammerl, G. Holl, T.M. Klapotke, P. Mayer, H. Noth, H. Piotrowski, M. Warchhold, Eur. J. Inorg. Chem. (2002) 834.
[13] J.C. Gálvez-Ruiz, G. Holl, K. Karaghiosoff, T.M. Klapötke, K. Löhnwitz, P. Mayer, H. Nöth, K. Polborn, C.J. Rohbogner, M. Suter, J.J. Weigand, Inorg. Chem. 44 (2005) 4237.
[14] H. Xue, Y. Gao, B. Twamley, J.M. Shreeve, Inorg. Chem. 44 (2005) 5068.
[15] R.P. Singh, R.D. Verma, D.T. Meshri, J.M. Shreeve, Angew. Chem., Int. Ed. 45 (2006) 3584.
[16] R. Wang, H. Gao, C. Ye, B. Twamley, J.M. Shreeve, Inorg. Chem. 46 (2007) 932.
[17] E. Lieber, E. Sherman, R.A. Henry, J. Cohen, J. Am. Chem. Soc. 73 (1951) 2327.
[18] A. Gao, A.L. Rheingold, T.B. Brill, Prop. Explos. Pyrotech. 16 (1991) 97.
[19] A.M. Astahov, R.S. Stepanov, L.A. Kruglikova, A.A. Nefedov, Russ. J. Org. Chem. 37 (2001) 611.
[20] B.C. Tappan, R.W. Beal, T.B. Brill, Thermochem. Acta 388 (2002) 227.
[21] Z.X. Chen, J.M. Xiao, H.M. Xiao, Y.N. Chiu, J. Phys. Chem. A 103 (1999) 8062.
[22] Z.-X. Chen, H. Xiao, Int. J. Quantum Chem. 79 (2000) 350.
[23] A.D. Vasiliev, A.M. Astakhov, A.A. Nefedov, R.S. Stepanov, J. Struct. Chem. 44 (2003) 322.
[24] A.M. Astakhov, A.D. Vasiliev, M.S. Molokeev, A.M. Sirotinin, L.A. Kruglyakova, J. Struct. Chem. 45 (2004) 175.
[25] B.C. Tappan, C.D. Incarvito, A.L. Rheingold, T.B. Brill, Thermochem. Acta 384 (2002) 113.
[26] A.M. Astakhov, A.D. Vasiliev, M.S. Molokeev, J. Struct. Chem. 45 (2004) 537.
[27] A.M. Astakhov, A.D. Vasiliev, M.S. Molokeev, A.M. Sirotinin, L.A. Kruglyakova, J. Struct. Chem. 45 (2004) 360.
[28] A.G. Mayanc, V.S. Klimenko, V.V. Erina, K.G. Pireseva, S.S. Gordeichuk, V.N. Leibzon, V.S. Kuzmin, Y.N. Burcev, Chim. Getcyc. Comp. (1991) 1067.
[29] S.F. Palopoli, S.J. Geib, A.L. Rheingold, T.B. Brill, Inorg. Chem. 27 (1988) 2963.
[30] A. Henry, R.C. Makosky, G.B.L. Smith, J. Am. Chem. Soc. 73 (1951) 474.
[31] H. Gilman (Ed.), Organic Syntheses, Russian Translation, vol. 1, Moscow, 1949, p. 298.
[32] J.P. Perdew, K. Burke, M. Erzenhorf, Phys. Rev. Lett. 77 (1996) 3865.
[33] J.P. Perdew, K. Burke, M. Erzenhorf, Phys. Rev. Lett. 78 (1997) 1396.

[34] C. Adamo, V. Barone, J. Chem. Phys. 110 (1999) 6158.
[35] A.A. Granovsky. Available from: <http://lcc.chem.msu.ru/gran/gamess/index.html>.
[36] M.W. Schmidt, K.K. Baldridge, J.A. Boatz, S.T. Elbert, M.S. Gordon, J.H. Jensen, S. Koseki, N. Matsunaga, K.A. Nguyen, S. Su, T.L. Windus, M. Dupuis, J.A. Montgomery, J. Comput. Chem. 14 (1993) 1347.
[37] A.E. Reed, L.A. Curtiss, F. Weinhold, Chem. Rev. 88 (1988) 899.
[38] F. Weinhold, C.A. Landis, Valency and Bonding: A Natural Bond Orbital Donor–Acceptor Perspective, Cambridge University Press, Cambridge, 2005, 760p.
[39] http://www.chemcraftprog.com.
[40] R.G. Pearson, Chemical Hardness: Applications from Molecules to Solids, Wiley–VCH Verlag GmbH, Weinheim/New York, 1997, 198p.
[41] E.J. Baerends, O.V. Gritsenko, R. van Leeuwen (Eds.), Chemical Applications of Density Functional Theory, ACS Symposium Series No. 269, vol. 20, American Chemical Society, 1996, p. 20.
[42] R. Stowasser, R. Hoffmann, J. Am. Chem. Soc. 121 (1999) 3414.
[43] R.G. Bryant, V.P. Chacko, M.C. Etter, Inorg. Chem. 23 (1984) 3580.
[44] P.J. Hagrman, D. Hagrman, J. Zubieta, Angew. Chem., Int. Ed. 38 (1999) 2638.
[45] J. Xianglin, S. Meicheng, H. Haochuan, W. Jinming, Z. Yu, Huaxue Tongbao (Chin.) (Chem. Bull.) (1982) 336.
[46] R.D. Shannon, Acta Crystallogr., Sect. A 32 (1976) 751.